

BAD STARS*

Richard A. Fowell,[†] Noah H. Smith,[‡] Sungkoo Bae,^{} Bob E. Schutz^{††}**

It is common to discover post-launch that some of the “eternal fixed stars” are not the reliable beacons one expected. The star tracker may frequently, or always, fail to acquire them. The positions reported by the star tracker may be biased or noisy. Such stars have been called “bad stars”. We report our findings from a “bad star” survey covering almost all of the celestial sphere, using the publicly available archive of ICESat star tracker in-flight measurements. The data is from three 10 Hz 8x8 deg FOV trackers from two vendors with complementary 3-axis gyro data. Tens of millions of 10 Hz star tracker measurements were analyzed, and nearly half the sky was scanned by both star tracker types. We compare the positions and magnitudes actually seen against those predicted in the published flight star catalog for the Aura spacecraft. We complement our findings with a literature survey of the topics: previously published “bad stars”, root causes, removal of star tracker measurement errors, and methods for identifying “bad stars”.

INTRODUCTION

On November 27, 2001, after nearly six years of operation, the NASA RXTE satellite went to inertial hold due to an attitude anomaly attributed to a “bad star”,¹⁻², a little over a year after a similar loss of star lock on September 6, 2000²⁻³. On July 30, 2003, the primary star tracker on Mars Express lost star lock, failed automatic reacquisition, and failed over to the secondary tracker due to a “bad star”³¹. In March 2001, after nearly 11 years of operation, five of 98 FHST (Fixed Head Star Tracker) updates attempted by the Hubble Space Telescope failed due to “bad stars” in the FGSSs (Fine Guidance Sensors)⁴. From 2000-2004, 444 attitude disturbances on the Chandra satellite were attributed to “bad stars”⁵. Clearly, there is room for improvement.

The term “bad star” dates back at least to May 1992, when the Hubble Space Telescope program had created a “bad star list” of guide stars that could not be acquired, or, worse, resulted in the star tracker reporting a different position than expected⁶⁻⁷. By October, 2000, there were thirty-two stars on the list, and three candidates for addition⁷.

“Bad stars” aren’t actually malevolent, of course. One problem is that the source data used to create CCD star tracker (CCDST) flight star catalogs was not collected for that purpose, but rather for astronomical science⁷⁻⁸. The standard process for creating a star catalog begins with astronomical position and brightness data taken by telescopes with subarcsecond level resolution through standard astronomical

* Copyright © 2008-2009 Boeing, Noah H. Smith, Sungkoo Bae, Bob E. Schutz. Published by the American Astronautical Society with permission. Permission is granted for nonprofit educational uses of this article. All other uses require permission from the copyright holders.

† Boeing Technical Fellow, Boeing, P.O. Box 92919, MC El Segundo, California 90009.

‡ Graduate Student, Center for Space Research, University of Texas at Austin, Texas 78712.

** Research Assistant/Engineer, Center for Space Research, University of Texas at Austin, Texas 78712.

†† Professor and Associate Director, Center for Space Research, Univ. of Texas at Austin, Texas 78712.

passband color filters⁸. For flight star catalogs, we would rather know how the sky appears to CCDSTs, which are deliberately defocused to several arcminute resolution, and respond over a broad silicon passband⁸. Methods of various levels of sophistication are used to compensate for these differences, but the final result is not as satisfactory as it might be⁸. NASA's SKY2000 Version 5 Master Catalog was developed as a source catalog from which to create flight star catalogs, and contains photometric data in the CCDST passband from CCDST flight data⁸. However, even SKY2000 Version 5 does not contain all stars typical CCDSTs can acquire, much less all the stars that might perturb the apparent positions of acquirable stars when viewed by a CCDST⁸. SKY2000 also has no information on the variability of the stars in the CCDST passband^{3,8}.

We think that CCDST flight star catalog quality can be improved by compiling source data comprised of direct measurements of apparent star positions and brightness using representative CCDSTs – by test rather than by analysis, if you will. Until recently, it has been difficult to get suitable source data. However, for many years now, NASA has been posting CCDST telemetry from the ICESat satellite on the National Snow and Ice Data Center (NSIDC) web site³⁴. The NSIDC web site now has over 2 billion publicly accessible CCDST measurements of over 8,000 stars taken over five years. This data can be used to determine apparent star positions to sub-arcsecond accuracy, and improve estimates of star brightness variability in the CCDST passband.

BACKGROUND

Process for creating flight star catalogs

Flight star catalogs for CCDSTs are tailored to the CCDST in question, and depend on the CCDST spectral response, field of view, pixel size, limiting magnitude, and other properties⁹. The approach taken by the French national space agency, CNES, is summarized in the 3 page flowchart, Figure 8.5.2.1 of Ref. 9. Fig. 2 of Ref. 10 is a more abbreviated flowchart of the approach taken for the Earth Observation System AM1 (EOS-AM1) satellite. The development of the 196,087 star guide star catalog for the Spitzer Space Telescope is detailed in Ref. 11.

The process begins with databases of astronomical objects. NASA's flight star catalogs¹² often use the SKY2000 Master Catalog¹³⁻¹⁸, sometimes augmented by the Tycho-1 catalog⁹. (SKY2000 was designed to support star sensor flight catalog work, but even Version 5 is believed to be missing some stars acquirable by a Ball CT-602 star tracker, and many that may perturb the centroids of acquirable stars⁸.) The European Space Operations Centre has proposed to use the Hipparcos and Tycho catalogs as the primary sources, together with the Hubble Guide Star Catalog and an independent master catalog of extended celestial objects¹⁹. For the Spitzer catalog, with guide stars as faint as magnitude 11, many catalogs were used¹¹. These included the Tycho, Tycho-2, Hipparcos, and Tycho Double Star catalogs, and the 2 Micron All Sky Survey Point Source Catalog (2MASS PSC), the US Naval Observatory A2.0 (USNO A2.0) catalog, the 2MASS Extended Source Catalog (2MASS XSC), the Principal Galaxy Catalog (2003) (PGC2003) and the Digital Sky Survey (DSS).

A critical step in the process is to determine the apparent brightness in the star sensor passband. Stellar magnitude is a logarithmic brightness scale. An arbitrary intensity, E_0 , is taken as the reference, and the magnitude of other objects is then $M = -2.5 * \log_{10}(E/E_0)$. Astronomical measurements are often taken through color filters, so a subscript is added to denote the filter, e.g., M_v (or simply V) for the magnitude through a “visual” filter, and M_B (or simply B) for the magnitude through a blue filter. There are multiple, differing, filter systems, e.g.: the Johnson and Cousins filter systems¹⁷ - this depends on both the filter system used and the filter type. Vega, an A0V star, was once the reference point for M_v ($M_v=0$). In star tracker work, the apparent magnitude for the star tracker spectral response is commonly called M_I (or simply I)^{9,20,21}. The reference point chosen for M_I varies – stars of type A0V²¹ (RXTE, Landsat 7, SOHO)¹², G2V²² (TERRA)¹² and G0V⁸ (AQUA, AURA, SWAS)¹², have all been used as the reference star.

Determining M_I is challenging - Ref. 9 calls this “the most delicate step”, since star photometry is incomplete and inconsistent, and stellar radiation does not follow a simple black body law. This step is complicated by the fact that every tracker has a slightly different star tracker response curve, even trackers of the same make and model. Figure 1 of Ref. 22 compares the star tracker response curves of two Ball

CT-601 star trackers on EOS-AM1, and Figure 3 of Ref. 16 presents the response curve of the Ball CT-601 star tracker on RXTE. Figure 8.2.2a of Ref. 9 shows a nominal and actual response curve for a SED-12 star tracker, and Figure 1 of Ref. 23 shows the response curve of the Indian Resourcesat-1 star tracker response. The three Ball CT-601 curves are clearly distinct, and the two non-Ball tracker responses are distinctly different from each other and from the Ball trackers. Shuttle flight data of two Ball CT-611 star trackers showed a difference in reported magnitude of 0.14 M_i for the bluest stars and 0.27 M_i for red stars²⁴.

Computing M_i would be more straightforward, if tedious, if both the detailed sensor response curve and the detailed source curve were available – the one can be convolved with the other^{9,23}. However, source spectral curves are readily available for a relatively small number of stars, such as the 13-color photometry of 1380 bright stars by Johnson and Mitchell²³, and the 180 stars in the Gunn & Stryker catalog⁹. A typical approach is to compute M_i directly for a set of stars with detailed spectral data, or flight data²⁴, as the “truth data”, then derive an empirical fit from secondary characteristics. Such secondary data includes photometry in common astronomical wideband passbands, or the spectral class and luminosity class. There are many astronomical passbands, of which the blue, visual, red, infrared (B,V,R,I)⁹ and deep infrared (J,K)¹¹ are common. Second order polynomial fits on (B-V), (V-R), (V-I), spectral class and luminosity class, and a linear combination of Sky2000 red passband 1 (usually R) and red passband 2 (usually I) have all been used^{9,23}. These empirical fits tend to have a fair number of outliers, and these outliers have been a source of many “bad stars”¹⁹. From Ref. 19: “... there were many instances of stars being more than 0.3 magnitudes fainter than predicted from the ISO guide star catalog, resulting in a failure to acquire the guide star.”. Computing M_i for variable stars and optical doubles by this approach is particularly problematic^{9,23,28}.

Variable stars are problematic for many reasons⁹. First, there are undetected variables. It takes only a few measurements to establish the brightness of a non-variable star, but many more to even detect that a star is a variable star. One “bad star” on the Galileo spacecraft was Delta Velorum, one of the 50 brightest stars in the sky – brighter than Polaris, and one of the ~150 in the Galileo star scanner catalog. Since Delta Velorum is an Algol-type eclipsing binary, its variability is only for a few hours out of every 45 days, and was not publicly disclosed as variable until 2001²⁹. We expect the prevalence of undetected variables in fainter stars is higher. Second, it takes many measurements to characterize the range of brightness of a variable star, and this task is complicated by the fact that not all variable stars are periodic, and that some have periods of years^{8,9}. Finally, the spectrum of a variable star often fluctuates together with its magnitude, making secondary characteristics like B-V vary as well⁹. As a result, even when a star is known to be variable, and its variability characterized by astronomers, the variability in the CCDST passband may be unknown⁸.

Many empirical M_i fits have been published in the literature. Fig. 4 of Ref. 24 plots I-V vs. B-V for two CT-611s. Fig. 1 of Ref. 25 plots I- $M_{\text{HIPPARCOS}}$ vs. stellar class/subclass for a STAR1000 active pixel sensor with Jena optics, using a G0V reference. Fig. 2.2 of Ref. 26 shows predicted I-V vs. B-V for a calibration set, and Fig. 3.6 of Ref. 26 shows I-V vs. B-V for ground observations using two different thresholding schemes, with and without disregarding suspicious stars. Faint stars tend to have dimmer reported values of M_i than would be calculated purely from the spectral convolution, due to the energy discarded by thresholding (Ref. 27, Fig. 4, shows an effect of 0.5 M_i for faint stars). Fig. 1 of Ref. 21 plots I-V vs. B-V, and notes that the scatter increases rapidly as B-V increases past 1.2. Figure AA-3 of Ref. 35 plots (V- M_i) vs. B-V for the predicted Ball CT-601 M_i for RXTE (partly based on flight data). Two of these studies using flight data concluded that some of the star measurements corresponded to misidentified stars^{24,28}.

Given the estimated M_i , one looks for sources that will be useful pointing references for the onboard star catalog. The sources should not be too faint (lest they not be detected) nor too bright (due to saturation effects)⁹. Also, high variability stars are frequently culled, as are stars with insufficient data to accurately compute M_i ^{8,21,24,28,35}.

Then proximity is considered. If other sources are sufficiently close, the star tracker won’t resolve them, and the apparent brightness and position will be determined by multiple sources. Such nearby stars

have been called “near neighbor”⁷ stars or “polluting”⁹ stars. Sometimes no single neighbor is bright enough to create a significant disturbance, but the composite effect is significant. Such cases have been called “integrated magnitude spoilers”⁷. The neighbors need not be single stars – they can be open clusters, globular clusters, bright galaxies, or nebulae^{6,9}. SKYMAP 15190039 was placed on the Hubble “bad stars” list for problems attributed to the M5 globular cluster⁷.

Such “blended” stars may be useful catalog stars, but the accuracy of the “blended” position is degraded, since it now depends on the accuracy of the computed Mi of the components, unlike the position of a single source. If a component is variable, the centroid changes with the magnitude of the variable source. Ref. 8 discusses this situation in detail for “bad star” SKYMAP 17310145 on the NASA Aura satellite due to the neglected long term variable neighbor V04835 Sco. It covers the “center of light” (COL) calculations used to predict the positions of “blended” catalog stars, and the blended magnitude estimates performed by the Multi-Mission Catalog generation program [MMSCAT]. For the RXTE CT-601 star tracker catalog, NASA blended all sources within 120 arcseconds radius of the catalog star when blending³⁵.

Stars whose neighbors are intermittently resolved, (depending on the star pixel phase and background noise²⁷) should be avoided, since the reported position toggles between multiple positions. Rosetta on board catalog #1717 was such a bad star²⁷. It was the expected fusion of Hipparcos 77052 (HIP77052) with faint neighbors HIP77034 and HIP77043. The reported position dithered between three values: the expected fusion, that of one subgroup, and that of another subgroup²⁷.

When considering star catalog candidates whose neighbors can safely be counted on to be resolved, the concern is “misidentification”⁹. If a neighbor is close enough in space and in brightness to the candidate, there is the danger that the star tracker may acquire it instead of the candidate, and the attitude determination system may mistake it for the candidate⁹. Such neighbors have been called “spoilers”⁶. In evaluating such neighbors, one must consider what positional and magnitude residual checks will be done by the operational system, and what the operational attitude uncertainty may be.

Given this background, and some examples, we are in a better position to examine the examples of “bad stars” reported in the literature, and to begin our search for more.

“Bad Stars” reported in the literature

This section summarizes published “bad stars”. These are specific examples to be wary of, and trial cases for screening methods. We only list a few samples from the Hubble “bad star list”, since it is long, and freely available on the Web⁷. Similarly, we don’t list the 13 RXTE stars listed in Ref. 3, Table 1, (by RXTE OSC4 IDs) that were dimmer than expected, and not always acquirable, since Ref. 3 is downloadable.

Table 1 provides: the catalog number of the “bad star”, of the principal disturbing object, the date the “bad star” was reported (or date of the reference, if unknown), the number from the References section, and a “bad star” code . The codes used begin with those from the Hubble “bad star list”, and are augmented for other types.

The star catalog abbreviations are: HIP for Hipparcos, SM for SkyMap, TYC for Tycho. These catalogs are available online at CDS: <http://cdsweb.u-strasbg.fr/> .

The “bad star” type codes used in Table 1 are:

- NN: Near Neighbor – a faint nearby star changes the position/magnitude
- IMS: Integrated Magnitude Spoiler – a number of faint nearby stars disturb position
- NSO: Nonstellar Object – Nonstellar Object
- PP: “Ping-Pong” – intermittently resolved “blended star” leads to jitter
- SP: Spoiler – unexpectedly bright neighbor is acquired and misidentified
- MD: Magnitude too dim – star dimmer than expected, infrequently or never acquired
- MB: Magnitude too bright – star brighter than expected, rejected by magnitude test
- VD: Variable star too dim
- VB: Variable star too bright – variable star brighter than expected

Primary ID	Secondary ID	Type	Date	Reference
Delta Velorum	-	VD	2001	29
SM15190039	M5	NSO	5/11/92	7
SM17380016	NGC 6397	NSO/NN	12/17/94	7
SM4370037	-	IMS	11/17/92	7
SM9370022	-	IMS	4/26/93	7
SM16040108	SM16040128	NN	5/03/00	7
SM200104	SM200127	NN	1998	7
SM 19220121	SM 19230045	PP	10/1/99	7
SM17310145	HD158619	NN/VB	7/20/2004	8
HIP 77072	HIP 77034	PP	10/17/2005	27
HIP 74778	HIP 74750	PP	9/26/2007	30
HIP 52009	-	MD	9/26/2007	30
~97-106 stars	-	MD	9/26/2007	30
M _V 5.43 B-V1.9	-	MD	7/30/2003	31
Not stated	M8 variable	NN/VB	9/2000	3
SM 1070042	Variable	NN/VB	11/2001	3
~214 suspected		Various	3/15/2002	3
13 stars		MD	3/15/2002	3
HIP 26220	Orion Nebula + Trapezium	SP/IMS/NSO	5/1999	33

Table 1: Some “Bad Stars” Reported in the Literature

ANALYSIS APPROACH

Strategy

In this study, we use in-frame star tracker data from the publicly available ICESat GLA04 flight telemetry files from the National Snow and Ice Data Center (NSIDC) website. We forgo the use of gyro data for simplicity.

Sensors and Operating Environment

ICESat is a currently operating NASA low earth orbit satellite using a Ball BCP2000 spacecraft bus, launched January 12, 2003. ICESat is in a 94° inclined, 590 km altitude, 96.5 minute orbit with a 183 day nodal regression period (0.5° per day sidereal precession rate)⁴¹⁻⁴⁵. The main payload is the Geoscience Laser Altimeter System (GLAS) laser altimeter for monitoring ice sheet thickness. The ICESat/GLAS web page at the Center for Space Research, University of Texas: <http://www.csr.utexas.edu/glas/>, has background material on ICESat, including the 94 page Algorithm Theoretical Basis Document (ATBD) for

the Precision Attitude Determination (PAD)³², as does the NASA ICESat web site: (<http://ICESat.gsfc.nasa.gov/links.php>).

ICESat carries four star trackers. The Instrument Star Tracker (IST) is a ROSI (now Goodrich) HD-1003 star tracker. In the nominal attitude, the IST is pitched at 0.3° from zenith. The IST has an 8°x8° field of view (FOV), a M_I 6.2 sensitivity, a 512x512 pixel CCD, and tracks up to 6 stars, with 10 Hz updates⁴².

ICESat flies four different attitudes, depending on the sign and magnitude of the angle from the orbit plane to the sunline⁴³. When the sun is within 32 degrees of the orbit plane, ICESat flies in “airplane mode”, with the solar array drive axes perpendicular to the orbit plane. Otherwise, ICESat flies in “sailboat mode”, with the solar array drive axes in the orbit plane. Stars travel along the IST pixel rows or columns, in the positive or negative direction – four possibilities in all. The IST operates in “full field of view” (FFOV) mode - the star tracker autonomously acquires new stars as stars leave the FOV.

The Laser Reference Sensor (LRS) is a second, modified 10 Hz HD-1003 with 3rd party optics and baffle, to reduce the FOV to 0.5°x0.5° and increase the sensitivity to M_I 7.5. No LRS data is used in this paper.

The two Ball Star Trackers (BST1 and BST2) are 10 Hz Ball CT-602 trackers whose boresights point 30° on either side of the IST boresight. The CT-602 has the same CCD and optics as the CT-601 used on RXTE. The BSTs have 8°x8° FOVs, M_I 7.1 sensitivity, a 512x512 pixel CCD, and can track 5 stars simultaneously. The BSTs operate in directed field of view (DFOV) under control of the ICESat attitude control system.

ICESat uses Litton (now Northrop Grumman) hemispherical resonating gyros (a SIRU) sampled at 10 Hz. No SIRU data is used in this paper.

Solar wing drive stepping causes vibrations of up to 20 arcseconds amplitude pk-pk at approximately 1 Hz at the IST, but the amplitude is closer to 2.5 arcseconds when the sun is close to the orbit plane⁴³.

ICESat typically flies a fixed attitude with respect to the orbit frame. Exceptions include the seasonal attitude switches, and twice/day 5° off-nadir “ocean scan” calibration slews over the Pacific equator – both ascending and descending passes. These are 20 minute duration octagonal roll-pitch scans with a 3-5° radius). Additionally, “targets of opportunity” (TOOs) at angles up to 5° off nadir are sometimes tasked⁴³.

Flight Telemetry Database

A vast amount of ICESat flight telemetry is freely available online at NASA’s National Snow and Ice Data Center (NSIDC) (<http://nsidc.org/data/ICESat/index.html>). This database is useful for many attitude determination and attitude sensor studies.

The data is packaged into 15 data products (<http://nsidc.org/data/ICESat/data.html>). The product used here is the GLA04 (GLAS/ICESat L1A Global Laser Pointing Data) product (<http://nsidc.org/data/gla04.html>). Each GLA04 file, or “granule” contains two orbits of attitude data from the BST1, BST2, IST, LRS and gyro sensors, together with satellite attitude, ephemeris, and solar array angles. Since ICESat has roughly 15 orbits per day, there are about 7.5 granules per day. Each GLA04 granule includes a “browse” file - a five page summary report with over 100 summary plots and other statistics. The data are available via FTP, DVD, CD-ROM, DLT, or 8-mm tape, in scaled integer binary format, big-endian (UNIX) byte order. The page: http://nsidc.org/cgi-bin/get_metadata.pl?id=gla04 provides metadata and a list of related publications. FORTRAN and IDL tools for processing the data are provided at <http://nsidc.org/data/ICESat/tools.html> . The data can be accessed through the “Data Pool” service at NSIDC: http://nsidc.org/data/data_pool/ .

The NSIDC GLA04 data is in “campaigns” averaging 35 days long, typically a spring and fall campaign each year from spring 2003-2008, plus a summer 2005 campaign, for a total of 511 days of 10Hz data as of fall 2008. The periods are at http://nsidc.org/data/ICESat/laser_op_periods.html .

We have identified 8840 unique stars in this dataset. Of these, 5262 were sampled by BST1, 5533 by BST2, and 7320 by the IST. 4309 were sampled by the IST and BST1, 4498 by the IST and BST2, and

4490 by both BSTs. 4022 were sampled by all three trackers. In Figure 1, stars sampled by the IST/BST1/BST2 are plotted as squares/circles/crosses.

The gap in the star coverage centered at Right Ascension (RA), Declination (DE) of $(100^\circ, 23^\circ)$ is the sun stayout zone for the IST. The gaps centered at $(12^\circ, 0^\circ)$, $(110^\circ, 70^\circ)$ and $(190^\circ, 0^\circ)$ are due to the NSIDC GLA04 dataset only covering the laser campaigns – year-round data is available which closes all gaps for the BSTs and all but the first for the IST. Such a “year of Wednesdays” dataset was provided to several researchers by the NSIDC upon request.

The GLA04 product is grouped into six files, five of which have attitude information (only GLA04-4 and GLA4-05 were used in the current study):

GLA04-01 Laser Profile Array [From the laser altimeter]

GLA04-02 Laser Reference Sensor (modified HD-1003, 0.5° by 0.5° FOV, Mi 7.5)

GLA04-03 Gyro (SIRU)

GLA04-04 Instrument Star Tracker (IST) (10 Hz HD-1003)

GLA04-05 Ball Star Trackers 1 & 2 (BSTs) (10 Hz CT-602s)

GLA04-06 Spacecraft Position and Attitude (attitude, ephemeris, wing position).

Descriptions of the file formats are given at the NASA Wallops Flight Facility Geoscience Laser Altimeter System (GLAS) Software Development Team (SDT) Ground Data System Home Page:
<http://glas.wff.nasa.gov/>.⁴⁶⁻⁵¹

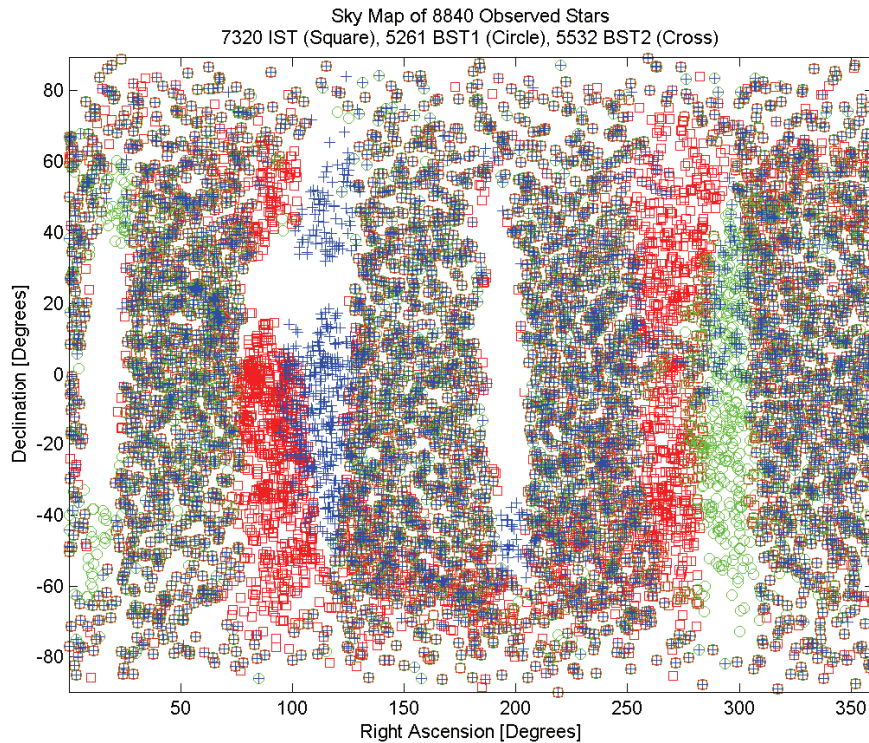


Figure 1: Locations of measured stars in the GLA04 dataset at NSIDC

The GLA04-04 (IST) data records are 1620 bytes each, with 35 fields, at 1 Hz. Of these, 24 fields are at 10 Hz (10 samples per record). For each of the six IST virtual trackers (VTs), the VT state, star valid flag, magnitude, encircled energy, H, V and background bias are provided at 10 Hz. The IST time to center

of integration, CCD temperature, lens cell temperature, effective focal length, boresight row, boresight column are also provided at 10 Hz.⁴⁹

The GLA04-04 Product Format Description gives the units as (arc-seconds * 100) for the IST H and V fields. This is a potential point of confusion, since raw HD-1003 H and V outputs are actually scaled tangents. However, the Product Format Description is correct – the HD-1003 outputs were converted from scaled tangents to angles as part of the GLA04 formatting for commonality with the BSTs.

The GLA04-05 (BSTs) data records are 2196 bytes each, with 56 fields. For each of the five VTs of each of the two BSTs, the star X position, Y position, and intensity are provided at 10 Hz. For each BST, the sample time, background reading, CCD temperature, baseplate temperature and lens temperature are provided at 10 Hz.⁵⁰

ICESat samples the IST and BSTs at their 10 Hz output rate, but the clocks are asynchronous with relative drift, so some star tracker frames are dropped.⁴¹

General Approach to Data Processing

This paper’s approach for improving flight star predictions for star apparent positions and to identify “bad stars” is to use the measured apparent “in-frame” separations from the star data from each star tracker individually. We do not try to fuse data from multiple star trackers, nor use the gyro data, though it is readily available.

The achievable accuracy from this type of approach is quite high – it has been argued that a “stellar only” approach to precision astrometry using block adjustment or iterative conventional adjustment is the best approach to precision astrometry⁵².

The average number of measurements per star in the NSIDC publicly available data is more than 250,000. If the star sensor measurement errors were independent, frame to frame, the apparent star positions could be recovered at the 50 milliarcsecond level. Correlated star tracker errors reduce the achievable accuracy, but with three star trackers, most stars traverse a star tracker field of view over 300 times in this dataset, and even brute force averaging should let us achieve a 160 milliarcsecond accuracy. Using “overlapping plate” methods to correct for systematic errors, we should be able to approach the 60 milliarcsecond level. Star variability and variation in spectral responsivity between star trackers will cause errors larger than this, of course.

Sixty milliarcseconds is unimpressive compared to the 2 milliarcsecond positional accuracies the Hipparcos catalog achieved at epoch. However, the Hipparcos precision is not directly applicable to conventional star sensor flight catalog centroids, which depend on background stars up to 120 arcseconds away³⁵. Conventional flight star catalog design guidelines implicitly tolerate near neighbor centroiding of 1.5 arcseconds or more⁸. “Center of Light”⁸ calculations can reduce these errors, but are subject to errors in the estimated CCDST magnitude of background stars – a 0.1 Mi error, 1 sigma, is typical, so COL might reduce 1.5 arcsecond errors to 150 milliarcseconds. Both the 1.5 arcsecond and 150 milliarcsecond values are for “good stars” - “bad star” outlier cases would be worse.

The present approach, besides being a way to detect “bad stars” at levels currently undetected, could improve apparent position accuracy up to 25-fold vs. the basic conventional approach, and 2-fold over COL techniques.

To achieve such accuracies, however, we need to address the issues of spurious measurements and star tracker errors.

By “spurious measurements”, we mean star centroids perturbed by CCD electrons caused by objects inside our solar system. These can be comets, asteroids, planets, planetary moons, satellites, debris, dust, proton strikes and “hot pixels” or “hot columns”.

Long-duration perturbations (comets, asteroids, planets, planetary moons) are typically handled by a priori, ephemeris based stayout zones for the planets, moons and brighter asteroids¹⁰.

“Hot pixels” or “hot columns” can be detected by trending star residuals as a function of CCD position⁴⁵, and ignoring measurements in the affected areas.

Spurious measurements that are essentially cases of the star tracker tracking satellites, debris or dust can be detected by checking for motion with respect to other stars.

Spurious measurements that are the overlap of objects with stars can often be detected and discarded by outlier removal based on positional and magnitude tests.

Star tracker errors are often categorized into temporal error (TE), high frequency error (HSF) and low spatial frequency error (LSF)⁵³.

Temporal error is uncorrelated frame-frame error. In our current approach, it is being addressed by calculating it on a star by star basis in time segments of a few seconds, and accounting for the measured noise in computing the measurement covariance.

High spatial frequency error (HSF) can be removed by modeling and/or notch filtering, but currently we simply measure it and account for it in the measurement covariance. It is of little consequence in the along-track direction, since averaging rapidly attenuates it. It is of most concern in the IST data, since the stars are traveling nominally along a row/column of the CCD, and the cross-track pixel phase is changing slowly at best, so HSF has a significant effect on the cross-track error for the IST. The stars move diagonally in BST row/column space, so averaging quickly attenuates BST HSF.

Low spatial frequency error is more troublesome, and the ICESat data reduction team decided in 2006 to perform plate modeling to remove the optical distortion effects⁴⁵.

Positional Data Processing

The positional uncertainty calculations, and outlier detection method used for this paper is the Mahalanobis approach, as used in the GAVO cross-matcher⁵⁵.

Each star (H,V) or (X,Y) measurement is corrected for low spatial frequency error using the plate model (Fig. 4) determined from in-flight measurements⁴⁵. The plate model is not currently a function of magnitude or temperature⁵⁶. The corrected angles are converted back to scaled tangents, and measured unit vectors are formed.

The star catalog unit vectors are corrected for velocity aberration and proper motion. Since parallax is less than 1 arcsecond, parallax is currently being ignored. The measured stars are identified from the measured star vectors. At this point, the star color can be determined, so chromatic aberration can be corrected, though this was not done here.

Each measurement vector is assigned a radial noise, then the transformation from the earth centered inertial frame (ECI) to the star tracker frame is calculated by solving the Wahba problem, and the 2x2 measurement covariance matrix is calculated from the radial noise numbers and the covariance formula for the Wahba problem.

An alternative approach is the “cloud” approach of Ref. 26, which uses the “bootstrap” method of solving for the attitude using subsets of the data, then looking at the statistics of the resulting population of results.

The radial noise is calculated by measuring the variance in each star pair separation over a few seconds, assuming each star has a constant radial position variance in that interval, and then solving the least squares solution for the radial position variance for each star³⁰. This approach works as long as there are at least three stars in the frame. For frames with fewer stars, the radial noise is estimated from the star magnitude using an empirically determined relationship between radial noise and star magnitude. Figure 2 shows such curves for the IST, BST1 and BST2. A star whose calculated noise is much different than expected is flagged for subsequent examination. It may be a transient, such as a satellite transit, or it may be an intermittently resolved “bad star”.

The high spatial frequency component is measured by computing the FFT of the difference between the star position and the expected position computed from the other stars in the frame. An example is Figure 3. By measuring the HSF, we can estimate how much of the apparent radial variance is due to HSF.

We want to examine each star to see if it has a biased position. One difficulty with standard residual test is that the estimate is biased by the biased star. We address this in this study with a process we refer to as “everyone’s a suspect”. More common terms for this type of outlier test are “leave-one-out residuals”, “Jackknife residuals”, “studentized residuals”, “externally studentized residuals”, “PRESS residuals”, “R-student residuals”, or “Quenouille-Tukey jackknife”.

“Jackknife” methods look at the statistics of subsets of $n-1$ samples of a population of n members, and “bootstrap” methods look at the statistics of subsets that may have fewer than $n-1$ samples. Ref. 27 suggests a “bootstrap” approach to determining the unbiased attitude: solving the Wahba problem for several small subgroups of the identified stars, and selecting the weighted median solution as the “truth” attitude.

In our approach, every star takes its turn as the “suspect” (hence, “everyone’s a suspect”). The attitude and the attitude covariance of each star tracker frame containing the current “suspect” star is calculated using the measurements of all the stars in that frame other than the suspect (the “jury”). For each frame, the jury’s calculated attitude and the star catalog unit vector for the suspect is used to calculate the expected position of the suspect in that frame. For each frame, the residual is calculated between the measured and the predicted position of the suspect. The residuals of all the frames in each transit of a star through a star tracker field of view are combined, averaged, and the covariance of the average is calculated from the attitude covariance of each frame. The Mahalanobis distance of the suspect star from the catalog distance is then computed from the average residual and the composite residual. Figure 5 is a histogram of our results.

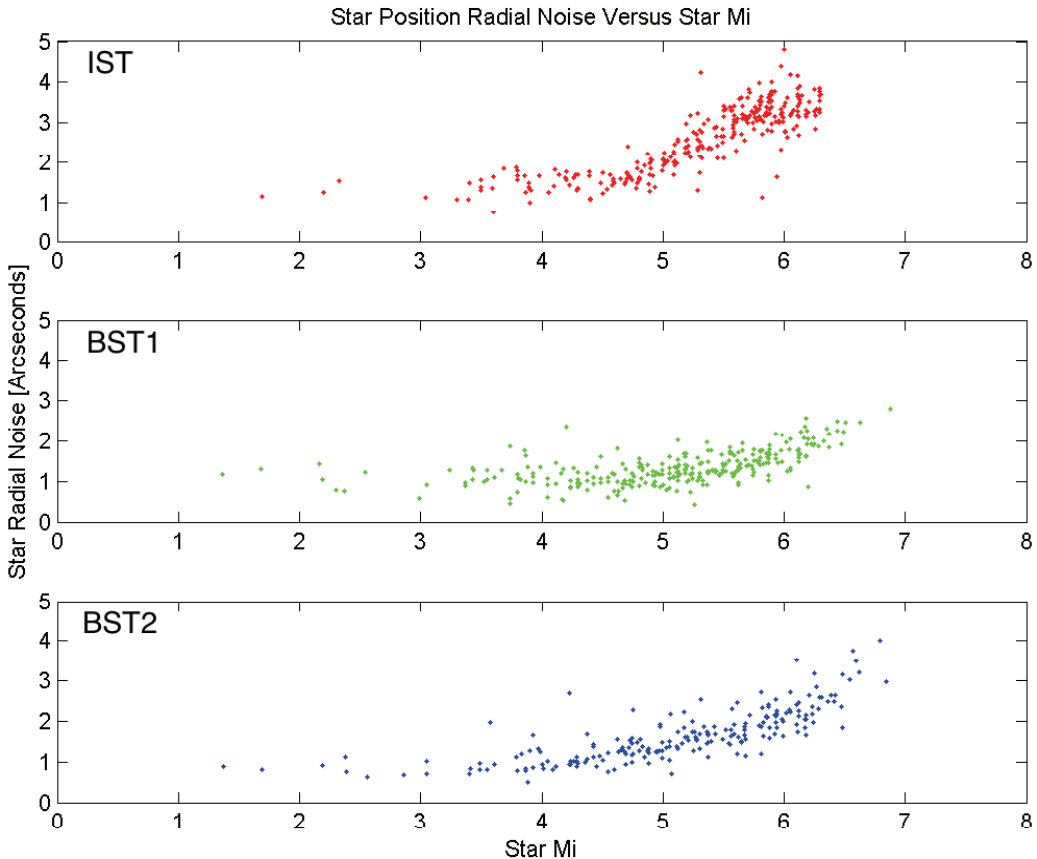


Figure 2: RMS radial noise in arcseconds vs. M_i for the three ICESat trackers

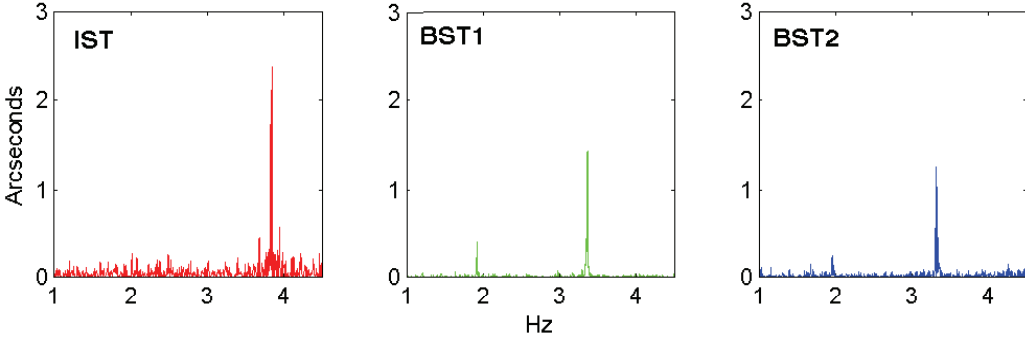


Figure 3: FFTs of Star Tracker Along-Track Residuals for an Mv 5.87 star (SkyMap 20500139)

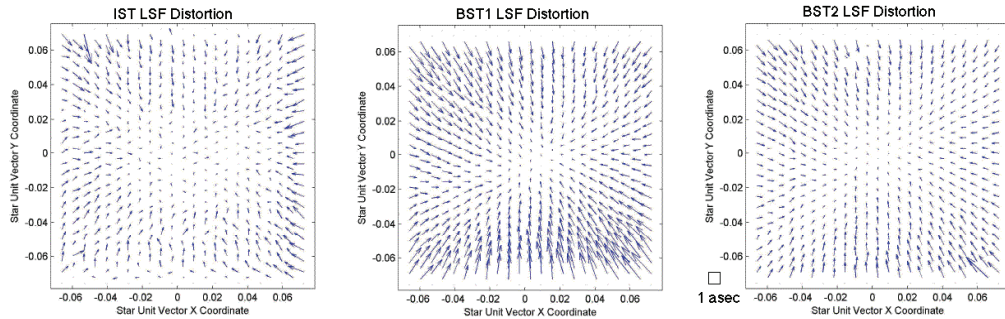


Figure 4: LSF Distortion Plots for the Three ICESat Star Trackers

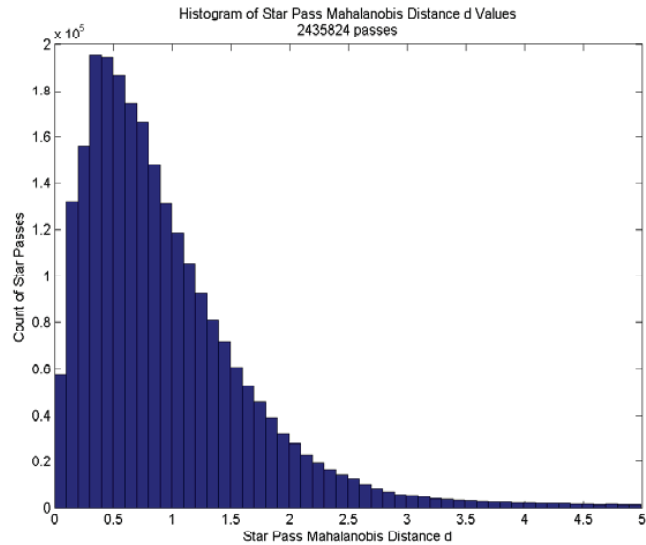


Figure 5: Histogram of Mahalanobis Distances for star passes (2.8% have d>5)

Stars with large Mahalanobis distances are examined in detail to distinguish truly “bad stars” from misidentifications or transient errors. Detailed error reports for each transit of a star through a star tracker field of view, or “pass”, are produced similar to those used on Chandra. If these reports do not exonerate the stars, we check astronomical data, including astrophotos of the sky within +/- 4 arcminutes of the star,

Figures 6-8 show three clearly displaced stars from the Aura on board catalog (OBC). The measured star positions are at left with the mean displacement in right ascension and declination. Each point plotted is the mean of the hundreds of star measurements in a pass. Shown at right are 8 x 8 arcminute red (R) passband astrophotos from STScI/MAST DSS, (© 1993-1995 Caltech/Palomar or © 1993-1995 AAO/ROE, as indicated).

The Aura documentation mentions that “center of light” positions were not computed, so some discrepancies were expected. However, in these three cases, the near neighbor is further from the catalog stars than the 120 arcseconds (2 arcminutes) that NASA cited as a CT-601 near neighbor criterion³⁵.

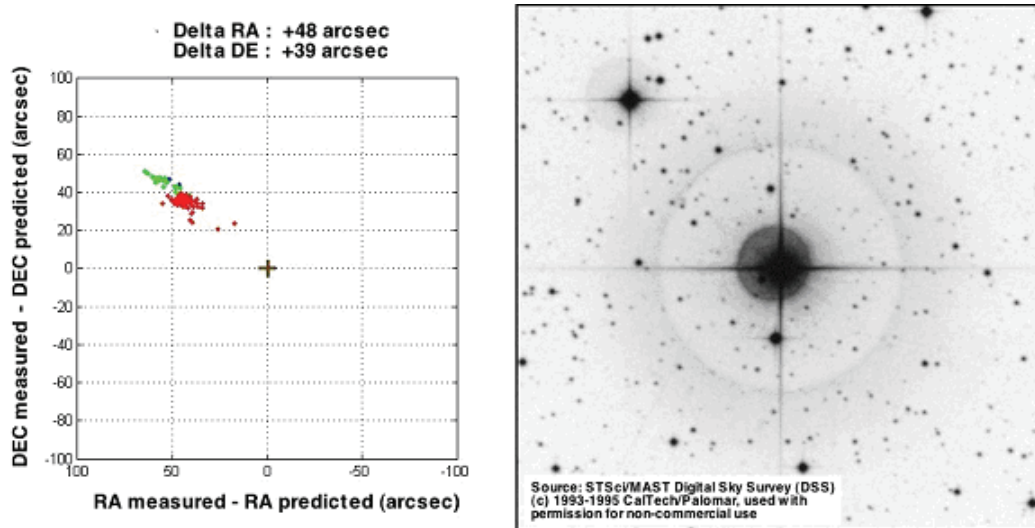


Figure 6: Aura OBC 3025 = HIP 115152 = SKYMAP 23190077

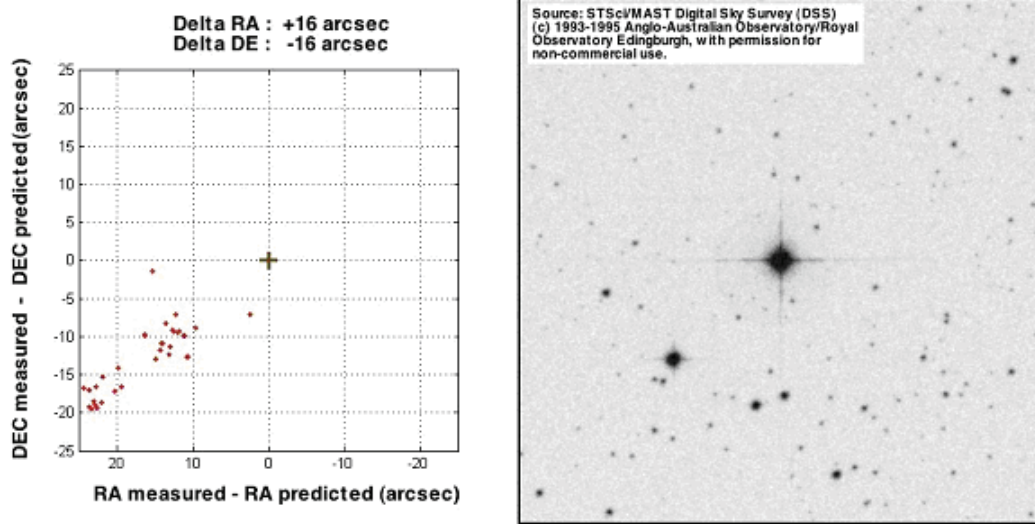


Figure 7: Aura OBC 759 = HIP 85786 = SKYMAP 17310145

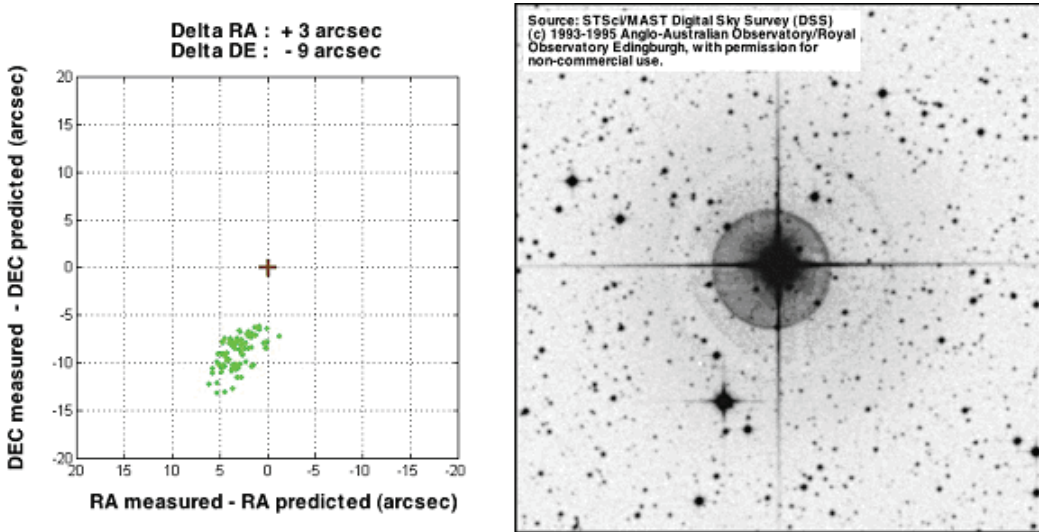


Figure 8: Aura OBC 1204 = HIP 96536 = SKYMAP 19370139

At the time of writing, we had only processed the ICESat data for “bad stars” with systematic mean offsets. “Ping-Pong” bad stars can have zero mean offset, but very large noise. Figure 9 shows a “ping-pong” bad star reported in Ref. 30. The two stars HIP 74778, HIP 74750 are alternately centroided singly or as a blend as a function of noise and pixel phase. The centroid toggles between three positions with time.

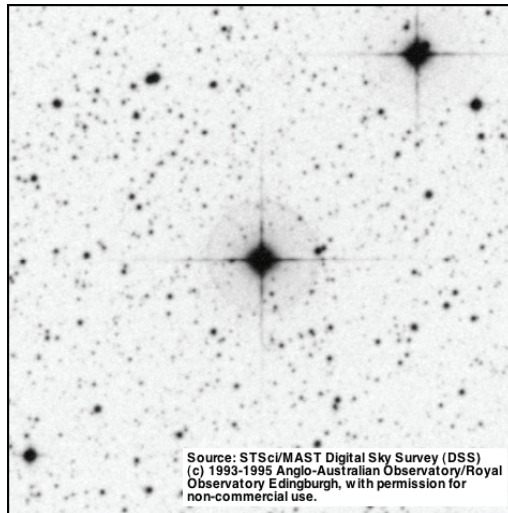


Figure 9: “Ping-Pong” “bad stars” HIP 74778, HIP 74750

Table 2 lists the Aura flight catalog IDs of 93 “good stars”. These are stars for which 20 or more passes were processed (300, on average), and whose average Mahalanobis distance was less than 0.5.

185 201 207 263 280 293 297 386 433 445 578 606 620 621 667 704 769 800 801 810 821 942
998 1110 1146 1148 1162 1169 1170 1176 1177 1188 1189 1190 1243 1251 1255 1266 1437 1497

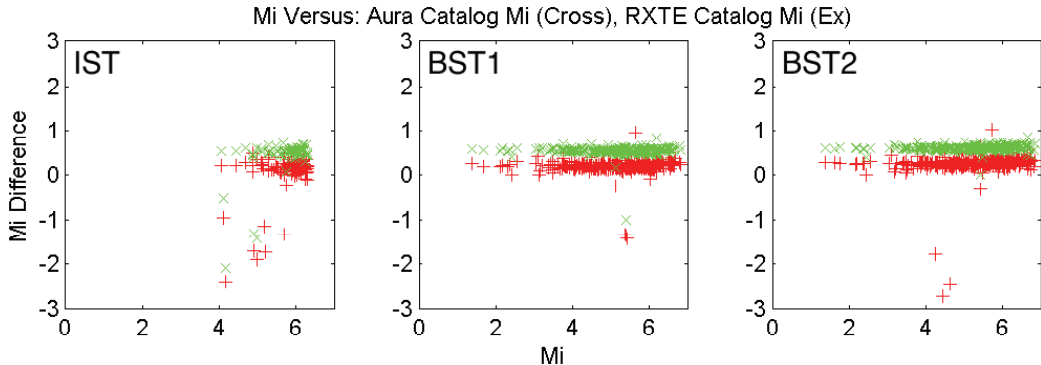
1571 1627 1628 1630 1644 1646 1651 1652 1679 1725 1728 1757 1924 1967 2051 2093 2114
 2117 2152 2176 2199 2408 2489 2500 2501 2503 2544 2558 2576 2613 2730 2799 2806 2821
 2831 2832 2836 2921 2925 2930 2934 2976 3008 3145 3154 3160 3179 3212 3261 3278 3281
 3298 3394

Table 2: “Good Stars”: AURA Catalog Stars with no Statistically Significant Deviation

Magnitude Data Processing

We have two good datasets for “expected” magnitudes from the NASA star catalog database¹². One is the Aura flight star catalog³⁸⁻⁴⁰ of 3542 stars, which presumably consists of stars that are selected to be well-behaved. The second is the dataset of RXTE flight-measured magnitudes³⁶⁻³⁷. This consists of 15,084 stars, and is not restricted to well-behaved stars. The RXTE dataset also includes some variable star information - the maximum and minimum observed magnitude in the CCDST passband. The IST, BST1 and BST2 observed magnitudes can be expected to deviate from the RXTE magnitudes due to tracker-tracker variation in response curve, and possibly different choice of reference star.

Our 8840 ICESat stars include 3171 (89%) of the Aura OBC, and 7014 (46%) of the RXTE database. 2771 are in both the Aura OBC and RXTE, and 400 are in the Aura OBC but not RXTE. 1826 ICESat stars are not in the RXTE database. We plan to summarize the flight measured magnitudes of the stars as observed by the IST, BST1 and BST2 in the same format as the RXTE data for a future paper. Figures 10-12 show the difference between the magnitudes measured on the three ICESat star trackers and the Aura and RXTE data, as a function of B-V.



Figures 10-12: ICESat Star Tracker Magnitudes minus RXTE and Aura OBC Catalog M_i.

CONCLUSIONS

Our examination of the publicly available ICESat GLA04 dataset has improved our understanding of the sky as viewed through 8x8 deg FOV, 512x512 pixel CCDs, and helped us improve the star catalog used to reduce the ICESat payload data. We feel that there is much more that can be learned from this dataset.

ACKNOWLEDGMENTS

The ICESat flight telemetry data used here came from the National Snow and Ice Data Center. The RXTE and Aura data came from the NASA Star Catalog Database¹². This research has made use of NASA's Astrophysics Data System : <http://www.adsabs.harvard.edu/>, the Aladin, SIMBAD and VizieR databases, operated at CDS, Strasbourg, France: (<http://aladin.u-strasbg.fr/>, <http://simbad.u-strasbg.fr/simbad/> , <http://webviz.u-strasbg.fr/viz-bin/VizieR>) and the Digital Sky Survey: <http://archive.stsci.edu/dss/> . Some of the data presented in this paper were obtained from the Multimission Archive at the Space Telescope Science Institute (MAST). STScI is

operated by the Association of Universities for Research in Astronomy, Inc., under NASA contract NAS5-26555. Support for MAST for non-HST data is provided by the NASA Office of Space Science via grant NAG5-7584 and by other grants and contracts.

REFERENCES

1. Baskill, Darren. Darren Baskill's Publications. 2008-10-16.
[URL: http://www.star.le.ac.uk/~dbl/publications/baavss3.html](http://www.star.le.ac.uk/~dbl/publications/baavss3.html) . Accessed: 2008-10-16. (Archived by WebCite® at <http://www.webcitation.org/5bcU3Goef>)
2. Markwardt, Craig. "RXTE Attitude Anomaly of September 6-12, 2000". October 2001.
[URL: http://lheawww.gsfc.nasa.gov/users/craigm/xteatterr/](http://lheawww.gsfc.nasa.gov/users/craigm/xteatterr/) . Accessed: 2008-10-16. (Archived by WebCite® at <http://www.webcitation.org/5bcVR9JSG>)
3. Sodano, Mr.. "Delivery of Updated Star Catalog for RXTE, Attachment: Delivery Documentation for the Updated RXTE Onboard. NASA Flight Dynamics Facility". 2002-03-15.
[URL: http://fdf.gsfc.nasa.gov/dist/generalProducts/attitude/ATT_rxte_osc6_delivery.pdf](http://fdf.gsfc.nasa.gov/dist/generalProducts/attitude/ATT_rxte_osc6_delivery.pdf) . Accessed: 2008-10-16. (Archived by WebCite® at <http://www.webcitation.org/5bcWeK8Fy>)
4. Anon., "Hubble Space Telescope Daily Report #2821. STSCI. 2001-03-05.
[URL: http://www.stsci.edu/ftp/observing/status_reports/old_reports_01/hst_status_03_05_01](http://www.stsci.edu/ftp/observing/status_reports/old_reports_01/hst_status_03_05_01) . Accessed: 2008-10-16. (Archived by WebCite® at <http://www.webcitation.org/5bcXH7hHb>)
5. Bucher, S; Martin, E. 2003:319 Attitude Disturbance. . 2004-06-29.
[URL: http://www.nasa.gov/offices/oce/llis/llis_lib/pdf/1011006main1_Flight_Note439_2003319_Attitude_Disturbance.pdf](http://www.nasa.gov/offices/oce/llis/llis_lib/pdf/1011006main1_Flight_Note439_2003319_Attitude_Disturbance.pdf) . (Archived by WebCite® 2008-10-16. at <http://www.webcitation.org/5bcZFnquo>)
6. Nadelman, M.S., Karl, Jeffrey B., "Fixed-Head Star Tracker Attitude Updates on the Hubble Space Telescope", Flight Mechanics/Estimation Theory Symposium, 1994, p 79-93, May 17-19, 1994.
<http://adsabs.harvard.edu/abs/1994fmet.symp...79N>
<http://hdl.handle.net/2060/19940031105>
7. McCutcheon, Bob. FHST Near Neighbor Problems and Integrated Magnitude Spoilers:. STSCI. 2000-12-12. [URL: http://ess.stsci.edu/sscb/web/dev/fgs_fhst_sup/phase3/nn_analysis_revised.txt](http://ess.stsci.edu/sscb/web/dev/fgs_fhst_sup/phase3/nn_analysis_revised.txt) . Accessed: 2008-10-16. (Archived by WebCite® at <http://www.webcitation.org/5bcctue8Z>)
8. Sande, Christopher B., Natanson, Gregory A., Treadwell, David A., "Effects of Uncataloged Near-Neighbor Stars on CCDST Operation", Flight Mechanics Symposium Goddard Space Flight Center Greenbelt, Maryland. [URL: http://www.aisolutions.com/file.asp?F=3DA865689C704F13A074999E41212161%2Epdf&N=Effects%5Fof%5FUncataloged%5FNear%2DNeighbor%5FStars%2Epdf&C=library](http://www.aisolutions.com/file.asp?F=3DA865689C704F13A074999E41212161%2Epdf&N=Effects%5Fof%5FUncataloged%5FNear%2DNeighbor%5FStars%2Epdf&C=library) . Accessed: 2008-10-16. (Archived by WebCite® at <http://www.webcitation.org/5bcnXSzI>)
9. Manon, F., "Astronomical References for Star Sensors", Chapter 8 of: Carrou, Jean-Pierre, *Spaceflight Dynamics*, Cepadues-Editions , 1995, Vol. 1, pp. 508-558.
10. Kudva, P., Throckmorton, A., "Preliminary star catalog development for the Earth Observation System AM1 (EOS-AM1) mission", Journal of Guidance, Control, and Dyn. 1996, vol.19 no.6 (1332-1336)
11. Van Bezooven, Roelof W. H.; Degen, Leo; Nichandros, Harry, "Guide star catalog for the Spitzer Space Telescope pointing calibration and reference sensor", Optical, Infrared, and Millimeter Space Telescopes. Edited by Mather, John C. Proceedings of the SPIE, Volume 5487, pp. 253-265 (2004),
<http://adsabs.harvard.edu/abs/2004SPIE.5487..253V>
12. Tracewell, David. Flight Dynamics' Star Catalog Database. NASA FDF
[URL: https://wakata.nascom.nasa.gov/dist/generalProducts/attitude/ATT_SKYMAP.html](https://wakata.nascom.nasa.gov/dist/generalProducts/attitude/ATT_SKYMAP.html) . Accessed: 2008-10-18. (Archived by WebCite® at <http://www.webcitation.org/5bfVD1j6s>)
13. Sande, C., Ottenstein, N., SKYMAP Requirements, Functional and Mathematical Specifications, Volume 3, Revision 3, (SKYMAP SKY2000 Version 2 Master Catalog Format Specifications), CSC-96-932-24, August 1999, Computer Sci. Corp,

[URL:\[https://wakata.nascom.nasa.gov/dist/generalProducts/attitude/ATT_sky2000_fmt.pdf\]\(https://wakata.nascom.nasa.gov/dist/generalProducts/attitude/ATT_sky2000_fmt.pdf\)](https://wakata.nascom.nasa.gov/dist/generalProducts/attitude/ATT_sky2000_fmt.pdf) . Accessed: 2008-10-19. (Archived by WebCite® at <http://www.webcitation.org/5bh1Gvurb>)

14. Sande, Christopher; . SKYMAP Sources and Data Representation, Version 5 Revision 4. Computer Sciences Corporation. 2008-10-19.
[URL:\[https://wakata.nascom.nasa.gov/dist/generalProducts/attitude/SKYMAP_Sources_and_Data_Representation_V5R4.pdf\]\(https://wakata.nascom.nasa.gov/dist/generalProducts/attitude/SKYMAP_Sources_and_Data_Representation_V5R4.pdf\)](https://wakata.nascom.nasa.gov/dist/generalProducts/attitude/SKYMAP_Sources_and_Data_Representation_V5R4.pdf),Archived by WebCite® 2008-10-29 at <http://www.webcitation.org/5bh24j8Zv>
15. Sande, Christopher; . Sky2000 Version 5. NASA. May 2006.
[URL:\[https://wakata.nascom.nasa.gov/dist/generalProducts/attitude/ATT_sky2kv5.cat.gz\]\(https://wakata.nascom.nasa.gov/dist/generalProducts/attitude/ATT_sky2kv5.cat.gz\)](https://wakata.nascom.nasa.gov/dist/generalProducts/attitude/ATT_sky2kv5.cat.gz) . Accessed: 2008-10-19. (Archived by WebCite® at <http://www.webcitation.org/5bh2hpum0>)
16. Sande, C.B., Brasoveanu, D., Miller, A.C., Home, A.T., Tracewell, D.A., "Improved Instrumental Magnitude Prediction Expected from Version 2 of the NASA SKY2000 Master Star Catalog", AAS 98-362, : AAS/GSFC 13th Intl Symp. on Space Flight Dyn, Volume 2, 741-754,, May 11-15 1998.
17. "Recent Enhancements to and Future Plans for the SKY2000 Star Catalog", JAAVSO Volume 29, 2001, pp. 123-128, Presented at the 89th Annual Meeting of the AAVSO, October 28, 2000.
[URL:<http://www.aavso.org/publications/ejaavso/v29n2/123.pdf>](http://www.aavso.org/publications/ejaavso/v29n2/123.pdf) . Accessed: 2008-10-19. (Archived by WebCite® at <http://www.webcitation.org/5bh4Ml43A>)
18. Myers, J. R.; Sande, C. B.; Miller, A. C.; Warren, W. H., Jr.; Tracewell, D. A., SKY2000 Catalog, Version 4 (Myers+ 2002), VizieR On-line Data Catalog: V/109. Originally published in: Goddard Space Flight Center, Flight Dynamics Division (2002), 09/2001,
<http://adsabs.harvard.edu/abs/2001yCat.5109...0M>
<http://vizier.cfa.harvard.edu/viz-bin/VizieR?-source=V/109>
19. Batten, A.; Marc, X.; McDonald, A.; Schutz, A., "The Use of the HIPPARCOS and TYCHO Catalogues in Flight Dynamics Operations at ESO", Proceedings of the ESA Symposium 'Hipparcos - Venice '97', 13-16 May, Venice, Italy, ESA SP-402 (July 1997), p. 191-194,
<http://adsabs.harvard.edu/abs/1997ESASP.402..191B>
20. Davenport, Paul B., "The Approximation of Stellar Energy Distributions and Magnitudes from Multi-Color Photometry", NASA TM X-63185, Goddard Space Flight Center, April 1968, 13pp.
<http://hdl.handle.net/2060/19680013463>
21. Strunz, Harry C., Baker, Troy, Ethridge, David, "Estimation of stellar instrument magnitudes", Proc. SPIE Vol. 1949, p. 228-235, Sept. 1993. <http://dx.doi.org/10.1117/12.157085>
22. Kudva, P. Flight Star Catalog Development for EOS-AM1. NASA. 1997-03-24.
[URL:\[https://fdf.gsfc.nasa.gov/dist/generalProducts/attitude/ATT_EOSAM1_final_report.pdf\]\(http://fdf.gsfc.nasa.gov/dist/generalProducts/attitude/ATT_EOSAM1_final_report.pdf\)](http://fdf.gsfc.nasa.gov/dist/generalProducts/attitude/ATT_EOSAM1_final_report.pdf) . Accessed: 2008-10-20. (Archived by WebCite® at <http://www.webcitation.org/5bhd9eaoh>)
23. Singh, Vandana, Pullaiah, D., Sreenivasa Rao, J., T.H Shashikala, T.H., G. Nagendra Rao, G.,Jain, Y.K. and T.K.Alex, "Generation and Validation of On-board Star Catalog for Resourcesat – I Star Tracker", AIAA 2004-5391, AIAA/AAS Astrodynamics Specialist Conference and Exhibit 16 - 19 August 2004, Providence, Rhode Island
24. Barry, Karen, Hindman, Mark, Yates, Russell, "Application of Flight Data to Space Shuttle CCD Star Tracker Catalog Design", AAS 93-015.
25. Schmidt, U, Michel, KI, Airey, S.P., "Active Pixel Sensor Technology Applied in Autonomous Star Sensors – Advantages and Challenges", AAS 07-063, G&C 2007, February 3-7, 2007, Breckenridge.
26. Kruijff, M., Heide, E.J. v.d. , de Boom, C.W., Heiden, N. v.d., "Star Sensor Algorithm Application and Spin-Off", IAC-03-A.5.03, 2003. [URL:<http://www.delta-utec.com/iaf/IAC-03-A.5.03-StarSensor-Kruijff.pdf>](http://www.delta-utec.com/iaf/IAC-03-A.5.03-StarSensor-Kruijff.pdf) . (Archived by WebCite® 2008-10-16 at <http://www.webcitation.org/5brqaea5E>)
27. Landi, A.; Boldrini, F.; Procopio, D., "Mars Express and Rosetta Autonomous STR: in Flight Experience", 6th International ESA Conference on GNC, held 17-20 October 2005 in Loutraki, Greece. ESA SP-606. European Space Agency, 2006
28. Anon. "Delivery documentation for the SKYMAP Aqua Star Catalog". 2002-04-10.
[URL:\[https://wakata.nascom.nasa.gov/dist/generalProducts/attitude/ATT_Aqua_StarCatalog_delivery\]\(https://wakata.nascom.nasa.gov/dist/generalProducts/attitude/ATT_Aqua_StarCatalog_delivery\)](https://wakata.nascom.nasa.gov/dist/generalProducts/attitude/ATT_Aqua_StarCatalog_delivery)

- [_041002.pdf](#) . (Archived by WebCite® 2008-10-26 at <http://www.webcitation.org/5brwUCF7J>)
29. NASA/JPL release. "Blinking star explains mystery aboard Galileo" Space News 2001-03-22.
[URL: http://spaceflightnow.com/news/n0103/22galblink/](http://spaceflightnow.com/news/n0103/22galblink/) . Accessed: 2008-10-26. (Archived by WebCite® at <http://www.webcitation.org/5bs6M5fLs>)
 30. Lauer, Mathias; Jauregui, Libe; Kielbassa, Sabine; "Operational Experience with Autonomous Star Trackers on ESA Interplanetary Spacecraft", in NASA/CP-2007-214158, 20th International Symposium on Space Flight Dynamics, 2007-09-26
[URL: http://fdab.gsfc.nasa.gov/live/Home/issfd2007/papers_dir/9-4Lauer.pdf](http://fdab.gsfc.nasa.gov/live/Home/issfd2007/papers_dir/9-4Lauer.pdf) . Accessed: 2008-10-26. (Archived by WebCite® at <http://www.webcitation.org/5bsHH711r>)
 31. Jayaraman, Pattam; Fischer, Joerg; Lauer, Mathias; Moorhouse, Allan; "Star Tracker Operational Usage in different phases of the Mars Express Mission 55860.doc, AIAA 2006-5930, SpaceOps 2006 .
 32. Bae, Sungkoo; Schutz, Bob E. "Geoscience Laser Altimeter System (GLAS) Algorithm Theoretical Basis Document Version 2.2 Precision Attitude Determination (PAD)". Center for Space Research. 10/2002. [URL: http://www.csr.utexas.edu/glas/pdf/atbd_pad_10_02.pdf](http://www.csr.utexas.edu/glas/pdf/atbd_pad_10_02.pdf) . Accessed: 2008-11-02. (Archived by WebCite® at <http://www.webcitation.org/5c1asETBM>)
 33. Kirschner, S.; Sedlak, J.; Challa, M.; Nicholson, A.; Sande, C.; Rohrbaugh, D., "Submillimeter Wave Astronomy Satellite (SWAS) Launch and Early Orbit Support Experiences", Flight Mechanics, Greenbelt, MD, 1999. <http://hdl.handle.net/2060/19990039118>
 34. Zwally, H.J., R. Schutz, C. Bentley, J. Bufton, T. Herring, J. Minster, J. Spinhirne, and R. Thomas. 2003, updated 2008. GLAS/ICESat L1A Global Laser Pointing Data V028/V029, ?? Feb ?? to ??Nov ???. Boulder, CO: National Snow and Ice Data Center. Digital media.
 35. Anon.. "Delivery of Updated Star Catalog for RXTE, Attachment: Delivery Documentation for the Updated RXTE StarCatalogs". NASA Flight Dynamics Facility. 2000-11-27.
[URL: https://wakata.nascom.nasa.gov/dist/generalProducts/attitude/ATT_RXTE_StarCatalog_delivery.pdf](https://wakata.nascom.nasa.gov/dist/generalProducts/attitude/ATT_RXTE_StarCatalog_delivery.pdf) . Accessed: 2008-11-02. (Archived by WebCite® at <http://www.webcitation.org/5c1WERVgC>)
 36. Anon.. "ASCII RXTE CCDST Data File". NASA Flight Dynamics Facility (FDF). 2006.
[URL: https://wakata.nascom.nasa.gov/dist/generalProducts/attitude/ATT_rxte_ccdst_data_reduced.txt.gz](https://wakata.nascom.nasa.gov/dist/generalProducts/attitude/ATT_rxte_ccdst_data_reduced.txt.gz) . Accessed: 2008-11-02. (Archived by WebCite® at <http://www.webcitation.org/5c1WlQah7>)
 37. Anon.. "Format description for the RXTE CCDST data file". NASA Flight Dynamics Facility. 2006
[URL: https://wakata.nascom.nasa.gov/dist/generalProducts/attitude/ATT_rxte_ccdst_data_fmt.pdf](https://wakata.nascom.nasa.gov/dist/generalProducts/attitude/ATT_rxte_ccdst_data_fmt.pdf) . Accessed: 2008-11-02. (Archived by WebCite® at <http://www.webcitation.org/5c1WxdSeQ>)
 38. Anon.. "MS-DOS/Windows OBC subset of the Aura Star Catalog" . NASA FDF. 2004-05-12.
[URL: https://wakata.nascom.nasa.gov/dist/generalProducts/attitude/ATT_aura_alp_obe_subset.cat.gz](https://wakata.nascom.nasa.gov/dist/generalProducts/attitude/ATT_aura_alp_obe_subset.cat.gz) . Accessed: 2008-11-02. (Archived by WebCite® at <http://www.webcitation.org/5c1XPSkyo>)
 39. Anon.. "MS-DOS/Windows Aura Star Catalog". NASA Flight Dynamics Facility. 2004-05-12.
[URL: https://wakata.nascom.nasa.gov/dist/generalProducts/attitude/ATT_aura_alp.cat.gz](https://wakata.nascom.nasa.gov/dist/generalProducts/attitude/ATT_aura_alp.cat.gz) . Accessed: 2008-11-02. (Archived by WebCite® at <http://www.webcitation.org/5c1Xf8AfE>)
 40. Anon.. "MS-DOS/Windows Aura Star Catalog with OBC identifiers in place of SKYMAP numbers". NASA Flight Dynamics Facility. 2004-05-12.
[URL: https://wakata.nascom.nasa.gov/dist/generalProducts/attitude/ATT_aura_alp_obe_ids.cat.gz](https://wakata.nascom.nasa.gov/dist/generalProducts/attitude/ATT_aura_alp_obe_ids.cat.gz) . Accessed: 2008-11-02. (Archived by WebCite® at <http://www.webcitation.org/5c1XxPKM0>)
 41. Schutz, B. E., Bae, S., Smith, N., Sirota, J. M.. "Precision Orbit And Attitude Determination For ICESat". AAS-08-305.URL: http://noahhsmithe.googlepages.com/schutz_markley_2008_final.pdf . (Archived by WebCite® on 2008-11-02 at <http://www.webcitation.org/5c1cRXDHF>)
 42. Schutz, Bob E., "Geolocation for the ICESat Laser Altimeter", AAS 05-011, 28th AAS Rocky Mountain Guidance and Control Conference, Feb. 5-9 2005, Breckenridge, pp. 127-142.
 43. Yoon, SungPil, Bae, Sungkoo, Schutz, Bob E., "High Frequency Attitude Motion of ICESat", AAS 05-108, AAS/AIAA Flight Mechanics Jan 23-27 2005, Copper Mountain CO., pp. 117-131.
 44. Schutz, B. E.; Zwally, H. J.; Shuman, C. A.; Hancock, D.; DiMarzio, J. P.."Overview of the ICESat Mission". Geophysical Research Letters, Volume 32, Issue 21. 2005-11-02.
[URL: http://ICESat.gsfc.nasa.gov/publications/GRL/schutz-1.pdf](http://ICESat.gsfc.nasa.gov/publications/GRL/schutz-1.pdf) . Accessed: 2008-11-02. (Archived by WebCite® at <http://www.webcitation.org/5c1fjczlV>)
 45. Smith, Noah. "Localized Distortion Estimation and Correction for the ICESat Star Trackers".

- University of Texas at Austin. M.S. Thesis 2006. URL:<http://noahhsmith.googlepages.com/thesis.pdf> . Accessed: 2008-11-02. (Archived by WebCite® at <http://www.webcitation.org/5c1crTpHi>)
46. Anon.. “GLA04-01 Product Format”. NASA. 2006-05-12.
URL:http://wffglas.wff.nasa.gov/v54_products/home.html?ht_action=view_format&ht_obj_key=4982 . Accessed: 2008-11-03. (Archived by WebCite® at <http://www.webcitation.org/5c330VKMe>)
 47. Anon.. “GLA04-02 Product Format”. NASA. 2004-09-09
URL:http://wffglas.wff.nasa.gov/v54_products/home.html?ht_action=view_format&ht_obj_key=4983 . Accessed: 2008-11-03. (Archived by WebCite® at <http://www.webcitation.org/5c33HVvFq>)
 48. Anon.. “GLA04-03 Product Format”. NASA. 2008-11-03.
URL:http://wffglas.wff.nasa.gov/v54_products/home.html?ht_action=view_format&ht_obj_key=4984 . Accessed: 2008-11-03. (Archived by WebCite® at <http://www.webcitation.org/5c33fnFtP>)
 49. Anon. “GLA04-04 Product Format, GLA04 IST_MAIN”. NASA. 2003-04-02.
URL:http://wffglas.wff.nasa.gov/v54_products/home.html?ht_action=view_format&ht_obj_key=4985 . Accessed: 2008-11-03. (Archived by WebCite® at <http://www.webcitation.org/5c33yVEXo>)
 50. Anon. “GLA04-05 Product Format, GLA04_BST_MAIN”. NASA. 2003-07-02.
URL:http://wffglas.wff.nasa.gov/v54_products/home.html?ht_action=view_format&ht_obj_key=4986 . Accessed: 2008-11-03. (Archived by WebCite® at <http://www.webcitation.org/5c34IbXe1>)
 51. Anon.. “GLA04-06 Product Format, GLA04 SCP_MAIN”. NASA. 2003-04-02.
URL:http://wffglas.wff.nasa.gov/v54_products/home.html?ht_action=view_format&ht_obj_key=4987 . Accessed: 2008-11-03. (Archived by WebCite® at <http://www.webcitation.org/5c34ZpzKf>)
 52. Zacharias, N, Dorland, B, “The concept of a stare-mode astrometric space mission”, PASP 10/2006 <http://adsabs.harvard.edu/abs/2006PASP..118.1419Z> <http://arxiv.org/abs/astro-ph/0608286>
 53. Lam, Quang; Woodruff, Craig; Ashton, Sanford ; Martin, David; “Noise Estimation for Star Tracker Calibration and Enhanced Precision Attitude”, Information Fusion, 2002. Proceedings of the Fifth Intnl. Conf, V: 1, pp. 235- 242 <http://www.isif.org/fusion02CD/pdffiles/papers/M1C01.pdf> Accessed: 2008-11-03. (Archived by WebCite® at <http://www.webcitation.org/5c36YyTU2>)
 54. Ghezal, Mehdi; Polle, Bernard; Rabejac, Christophe; Montel, Johan; “Gyro Stellar Attitude Determination”, Proc. 6th ESA Conf. on GNC, Loutraki, Greece, 17-20 Oct. 2006 (ESA SP-606).
 55. Adorf, H.-M.; Lemson, G.; Voges, W.; Enke, H.; Steinmetz, M., “Astronomical Catalogues - Simultaneous Querying and Matching”, ADASS XIII, 12-15 October, 2003, Strasbourg, France. <http://adsabs.harvard.edu/abs/2004ASPC..314..281A>
 56. Thomas, V. C.; Blue, R. C.; Procopio, D.; Galileo, O., “Cassini Stellar Reference Unit: Performance Test Approach and Results”, 8/4/1996, Denver, Colorado, SPIE Vol. 2803, pp. 288-298, <http://hdl.handle.net/2014/26128>
 57. NM Gomes, M Fouquet and WH Steyn, “Astrolabe - A Low Cost Autonomous Star Camera”, 4th International Symposium on Small Satellites Systems and Services, Antibes France, 14-18 September 1998, Proceedings: Session 6/7., http://staff.ee.sun.ac.za/whsteyn/Papers/SSSS98_Star.pdf Accessed: 2008-11-03. (Archived by WebCite® at <http://www.webcitation.org/5c38t7C6o>)